Indian Journal of Pure & Applied Physics
Vol. 62, June 2024, pp. 510-516
DOI: 10.56042/ijpap.v62i6.6344

Graphite Carbon with a Nanofiber Structure Derived from Oil Palm Fiber Biomass for Active Material for Supercapacitor Cells

Dian Eka Rachmawati, Rakhmawati Farma*& Irma Apriyani

Department of Physics, University of Riau, Simpang Baru, 28293 Riau, Indonesia

Received 23 October 2023; accepted 12 April 2024

Biomass-based renewable energy sources have attracted the attention of researchers due to the long-term and large-scale use of fossil fuels globally. In this research, biomass from Oil Palm Fiber (OPF) was identified to be processed into active material for supercapacitor cells. Activation with the help of chemical regens from KOH, $NiCl_2$, and $ZnCl_2$ is carried out to obtain superior quality OPF active materials. Double pyrolysis was also carried out, carbonization of N_2 at 600 ℃ and physical activation of CO_2 at 800 ℃. The graphite structure is obtained with nanofibers and nanospheres and nanopores with anSSAof 591 m^2/g. These properties enable the OPF-N active material to obtain a specific capacitance of up to 255 F/g under 1M H_2SO_4 acid conditions with a scan rate of 1 mV/s. This research provides a new approach and scientific basis for the construction, design, and application of green energy storage devices.

Keywords: Graphite carbon; Nanofiber; Oil palm fiber; Active material; Supercapacitor

1 Introduction

Global energy consumption has increased, in 2015 energy consumption reached 575 quadrillion BTU (British Thermal Unit) and is expected to increase until 2040 to 736 quadrillion BTU[1]. Current energy sources, basically still rely on fossil fuels and are predicted to be unable to meet energy demand in the future. In addition, these fossil fuels have negative impacts, and a series of serious ecological crises, such as environmental pollution, the greenhouse effect, and extreme weather conditions[2]. There is a need to develop renewable energy-based energy as a solution to the global energy crisis and convert it into energy storage devices such as batteries, fuel cells, capacitors, and supercapacitors. Green or renewable energy sources are energy that have the characteristics of being environmentally friendly, efficient, clean, abundant, sustainable, and can be mass-produced at low cost. Several sources and types of renewable energy such as solar energy, geothermal, wind, hydropower, tidal, piezoelectric, and biomass, where biomass has a very superior role compared to others because it does not have time, weather, circumstances, and regional limitations.

Supercapacitor is an energy storage device with superior performance compared to batteries, capacitors, and fuel cells. Long supercapacitor life cycle with fast charge-discharge capacity and superior energy compared to capacitors as well as higher power than batteries and fuel cells[3]. The characteristics of the supercapacitor active material greatly affect its performance. Promising active materials for supercapacitor electrodes include conductive polymers, metal dioxide, and porous carbon (nanotubes, graphene, fullerene, activated carbon, and others). Activated carbon from biomass has high economic value, abundant availability, structural engineering of surface morphology, high carbon content, and is go-green[4]. Biomass-based supercapacitors are one of the focuses of researchers at this time, with ongoing development to find the potential of various biomass with the best quality for supercapacitor cell performance.

The biomass whose performance has been investigated as an active material for supercapacitor cells is the biomass of empty sugar palm fruit bunches[5], female palm coir[6], nipa coir[7], casuarina bark[8], coconut coir[9], areca nut coir[1], and in this research we will investigate palm fruit fiber. Indonesia is the largest palm oil-producing country in the world, where palm oil is produced into Crude Palm Oil (CPO) and Palm Kernel Oil (PKO) which are consumed demographically and exported to various other countries. Palm oil production in large quantities leads to the production of very large palm

*Corresponding author:
(E-mail: rakhmawati.farma@lecturer.unri.ac.id)

oil wastes such as palm fronds, oil palm trunks, empty palm oil bunches (EPOB), and oil palmfiber (OPF)[10]. Handling and utilization of palm oil industry waste is a phenomenal issue to turn it into a technology that is sustainable, environmentally friendly, and economical. OPF is a biomass that contains lignocellulosic with long carbon chains and high carbon content so that it can be used as a supercapacitor carbon material[11].

This research was conducted to develop a new technology for the utilization of biomass waste from the palm oil industry, namely OPF, to produce high-performance supercapacitor cell carbon electrodes by engineering the surface morphology structure and increasing graphitization[12]. The degree of graphitization is also one of the factors affecting the electrochemical performance of supercapacitors, not only increasing the electrical conductivity but also reducing the internal resistance and stabilizing the carbon structure. The ion diffusion rate is strongly influenced by the pore size, whereas fast electron transfer is closely related to good electrical conductivity. In general, pyrolysis temperature (>1000 °C) can make carbon atoms rearrange into conjugated sp^2-C atoms and achieve a well-developed graphite structure[13]. However, biomass-based carbon is a disordered carbon with diverse structures and morphologies, which is difficult to mutate into graphite structures even at a high temperature of 2500 °C. In addition, high temperature (>1000 °C) pyrolysis not only consumes a lot of energy but also breaks down many pores in carbon materials, resulting in an undeveloped pore structure and a small surface specific area (SSA). Catalytic graphitization is an effective strategy for converting amorphous carbon into graphite at low temperatures (≤1000 °C) by adding substances containing transition metal elements (Ni, Co, and Fe) to the carbon matrix. Furthermore, metal particles can also act as templates to form additional pores[12].

The integration of activated carbon derived from biomass with a $NiCl_2$ catalyst serves as a pivotal advancement in enhancing the functionality of Electric Double-Layer Capacitors (EDLC). This innovative mixture harnesses the porous structure of activated carbon, derived from sustainable biomass sources, to facilitate high surface area and efficient ion adsorption. The inclusion of $NiCl_2$ catalyst further augments the electrochemical performance by promoting charge transfer kinetics and improving the overall conductivity of the electrode material[14]. Consequently, this synergistic combination enables EDLC to achieve enhanced energy storage capacity, improved rate capability, and prolonged cyclic stability, thereby paving the way for more sustainable and efficient energy storage solutions across various applications, from portable electronics to renewable energy systems[15]. Researchers have previously succeeded in utilizing biomass waste as an electrode material for supercapacitors, researchers[16] synthesized carbon material from mushrooms with the addition of $FeCl_3$ as a catalyst material to obtain a specific capacitance (C_{sp}) of 247 Fg^{-1}. Researchers[17]also made carbon electrodes based on Cornstalk biomass waste with the catalyst $K_4[Fe(CN)_6]$ to obtain a C_{sp} of 213 Fg^{-1}. In this research, we have succeeded in providing active material from oil palm fiber using the catalyst $NiCl_2$ to obtain a Csp of 250 Fg^{-1}.

2 Experimentation

KOH, $ZnCl_2$, $NiCl_2$, HCl, H_2SO_4, and ethanol, were obtained from Sigma Aldrich. The scheme for making active material from oil palm fiber (OPF) and its application to supercapacitor cells can be seen in Fig. 1. OPF was obtained from PT. Oil Palm Industry, washed, soaked in hot water, then dried in the sun. To produce self-adhesive OPF powder with a size ≤ 53 μm, it was pre-carbonized at 200 ℃ for 1 h, then ball milled and sieved (53 μm). Activation or addition of chemicals was carried out on 30 g of carbon powder using KOH, $ZnCl_2$ and $NiCl_2$ and continued with the formation of carbon pellets using a press from a hydraulic press at a pressure of 7 tons. The most important process is the dual combustion or pyrolysis of the OPF carbon pellets. The first pyrolysis called the carbonization stage, was carried out under a nitrogen atmosphere at a temperature of 600 ℃ for 6 h18 min with a heating rate and flow rate of 3 ℃/min and 1.5 L/min respectively. The second pyrolysis or what is called the physical activation process is carried out under a carbon dioxide atmosphere at a temperature of 800 ℃ for 1 h20 minwith a heating rate and flow rate of 10 ℃/min and 1 L/min respectively. The active materials obtained were neutralized using distilled water until they reached a pH of ~7, and were named OPF-K, OPF-N and OPF-Z based on the chemical regens KOH, $NiCl_2$ and $ZnCl_2$. OPF active material having a mass of ≤ 0.005 g with a diameter of ≤7 mm and a thickness of ≤ 3 mm was immersed in 1M H_2SO_4 solution.

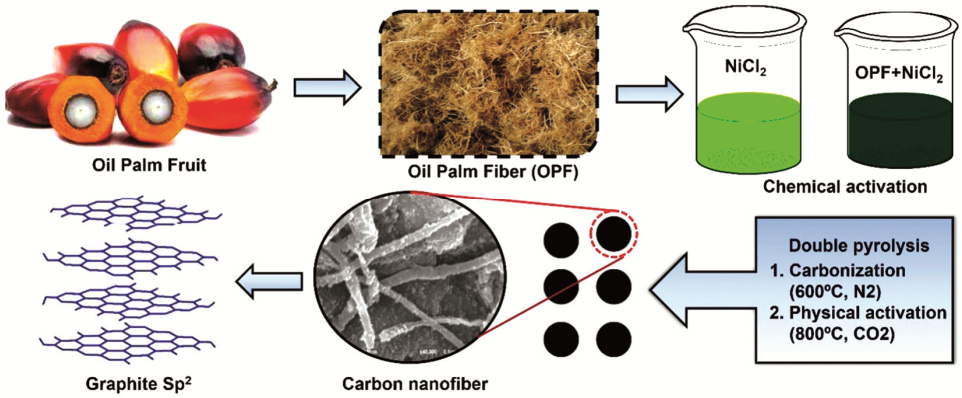

Fig. 1 — Scheme for making active materials from oil palm fiber

To analyze the effect of chemical regen on supercapacitor performance, physical properties tests were carried out which consisted of X-ray diffraction (XRD), Fourier Transform Infrared Spectroscopy (FTIR), scanning electron microscopy (SEM) and Energy Dispersive X-ray (EDX), Brunauer- Emmett-Teller (BET) and Barrett-Joyner-Halenda (BJH). The XRD test was carried out to determine the microcrystalline structure of the OPF active material using the Shimadzu 700 XRD instrument, while the FTIR test was carried out to determine the functional groups of OPF with the Shimadzu Prestige-21 IR instrument. Elemental analysis of C, O, and impurities in the OPF active material was carried out using the EDX test (0-10 keV) and OPF surface morphology analysis was carried out using the SEM test at 5000 and 40000 x magnification, SEM-EDX was carried out using the SEM-EDX instrument, JEOL JSM- 6510 LA. The SSA of the OPF was analyzed using the BET method and the pore size distribution was analyzed using the BJH method with the N2 isothermal adsorption desorption approach using the Quantachrome TouchWin v1.22 instrument (St 3 on NOVA touch 4LX). The capacitive performance of OPF active materials was tested, first using the cyclic voltammetry (CV) method and second, using Galvanostatic Charge Discharge (GCD). A symmetrical two-electrode OPF arrangement was created, and 1 M H_2SO_4 solution was used as the electrolyte. CV and GCD tests for OPF active materials, a voltage of 0-1 V was applied with varying scan rates and current densities, namely 1,2, 5, and 10 mV/s and 1,2,5,10 A/g.

3 Results and Discussion

3.1 Analysis of the Physical Properties of the OPF Active Material

The crystalline and amorphous phases of the OPF active material were identified using XRD analysis, the OPF active material revealed a semicrystalline structure, namely a combination of amorphous and crystalline. As seen in Fig. 2 (a), the amorphous structure is characterized by two gently sloping peaks present at an angle of 2θ around 24° and 44° corresponding to the crystalline planes of graphite carbon (002) and (100)[18]. The sharp peaks in the OPF-N and OPF-Z active materials reveal the presence of crystalline compounds at an angle of 2θ around 26° and 43° which are graphite peaks. Ni particles can also be used as a graphitization catalyst to promote the formation of graphitization structures. The graphite structure is very advantageous in transporting ions and increasing the electrical conductivity of the OPF active material which is consistent with better electrochemical properties[19]. Furthermore, the OPF-N active material also experiences the presence of impurities such as calcite $CaCO_3$, marked by a sharp peak at an angle of 2θ 50°. OPF-Z also has a sharp peak present around the 2θ 35° angle indicating carbon monoxide (CO), which is a colorless, odorless, and tasteless gas. It consists of one carbon atom covalently bonded to one oxygen atom. In this bond, there are two covalent bonds and one coordination covalent bond between the carbon and oxygen atoms. Carbon monoxide is produced from incomplete combustion of carbon compounds in the process of converting midrib palm oil biomass into active materials.

The process of activating the OPF material causes sp^3 C-X bonds, where X can be in the form of C, O, and H transitioning into sp^2 aromatic bonds. The presence of functional groups in the OPF active material was analyzed using the FTIR test, as seen in Fig. 2(b) at wave numbers 500-4500 cm^{-1}. The FTIR spectra of OPF-K, OPF-N, and OPF-Z have similar absorptions. The FTIR spectrum in the

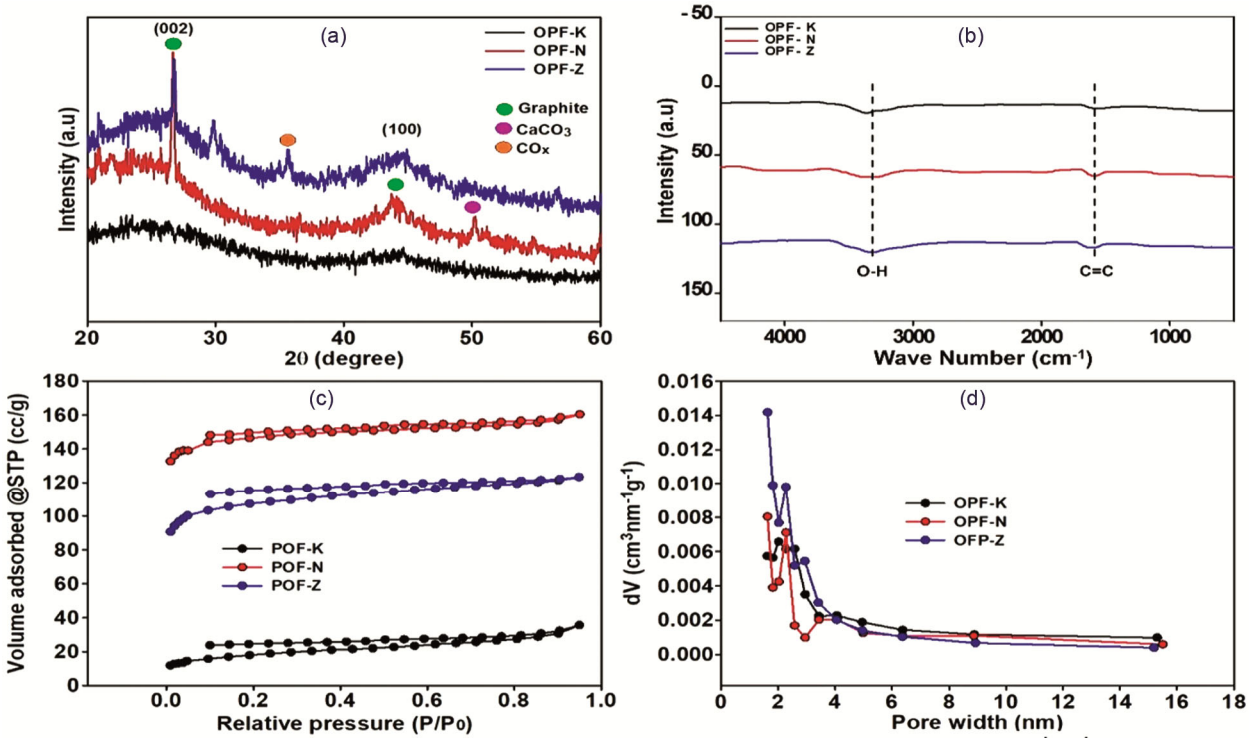

Fig. 2 — (a) XRD spectral pattern, (b) FTIR spectral pattern, (c) adsorption-desorption isothermal N_2, (d) pore size distribution

3300-3650 cm-1 peak is related to the hydroxyl O-H functional group, which can improve the electrochemical properties of the material[20]. The band peak also occurs at wave number 1629 cm^{-1} which is related to the tensile vibration of the C=C double carbon bond or the benzene ring bound to sp[2[21]].

Figure 2(c) shows the N_2 adsorption-desorption isothermal curve of the OPF active material based on the chemical activation of KOH, $NiCl_2$, and $ZnCl_2$. All OPFs have a type IV isothermal curve according to the IUPAC isotherm classification[22]. The active material increases sharply in the relatively low-pressure region ($P/P_0<0.1$) due to the presence of abundant micropores. At pressure ($0.4 < P/P0 < 0.9$) an H3-type hysteresis loop is formed indicating a rich mesopore. The highest N_2 isothermal adsorption-desorption is owned by OPF-N, which means that the active material absorbs and releases nitrogen in greater quantities, and exhibits better porosity quality and a greater amount. The SSA of each OPF active material is 65, 591, and 422 m2/g for OPF-K, OPF-N and OPF-Z. Nicl2 activator has succeeded in forming a superior pore structure so that it has a high SSA compared to OPF-K and OPF-Z.

Figure 2(d) shows the pore size distribution of the OPF active material which consists of 1.62 nm-1.81 nm micropores and 2.02 nm-15.3 nm mesopores. Most of the pores are of mesopore origin (2 to 15.3 nm), although micropores (2.02 to 15.3 nm) are present. Overall, the average pore diameter is about 2.3 nm, a porous structure[23]. The Electrochemical double-layer capacitor (EDLC) charge storage mechanism employs electrostatic interactions, which can be enhanced in materials that have a high SSA and are highly porous. Various types of pores, and electrolyte ions can permeate throughout the material so that it is exposed to the maximum active SSAother than the pore walls, which results in the maximum charge-discharge process of the supercapacitor. This suggests that OPF-N will serve well as an effective electrode material for symmetric supercapacitors, especially due to its high SSA and porous[24].

The surface morphology of the OPF active material was investigated through SEM characterization and the results are presented in Fig. 3. Figures. 3(a & b) are the surface morphology of the OPF active material activated with the help of KOH, showing aggregates with less porosity and nanofibers. Activation of $NiCL_2$ on OPF produces a greater number of nanofibers and the formation of nanospheres with more porosity. $NiCl_2$ can evaporate hydrocarbon compounds, volatiles, and impurities from biomass, where the evaporation of cellulose plays a role in the formation of nanofibers and the evaporation of lignin

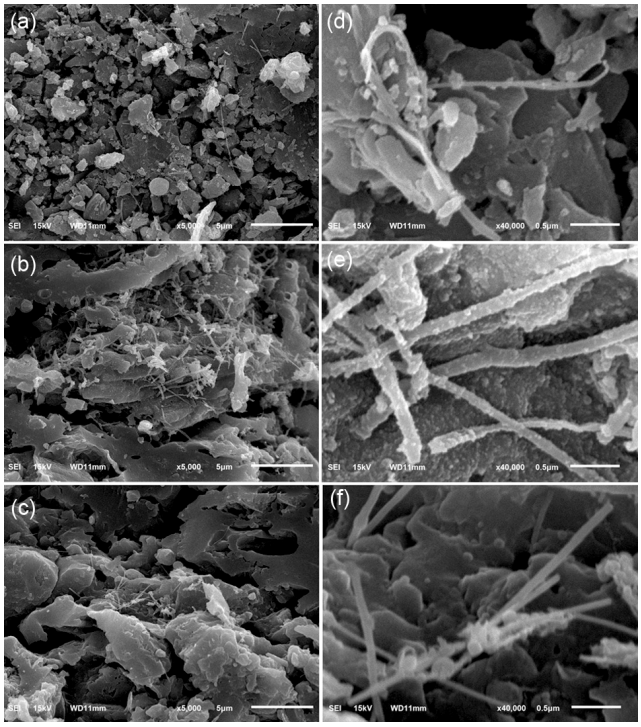

Fig. 3 — SEM micrographs magnification 5000 x (a) OPF-K, (b) OPF-N, (c) OPF-Z, magnification 40000 (d) OPF-K, (e) OPF-N, and (f) OPF –Z

and hemicellulose plays a role in the formation of nanospheres and nanopores. Nanofibers can reduce the movement distance of ions and provide a larger electrode-electrolyte contact area and a flexible substrate[25,26]. The active material OPF-Z has a nanofiber structure with aggregates with a porosity that is not much different from OPF-K. OPF-N has significantly more nanofibers than OPF-K and OPF-Z indicating better electrochemical properties which will be confirmed by CV analysis.Furthermore, nanofiber structures embedded with aggregates and possessing porosity play a pivotal role in enhancing the performance of supercapacitors, specifically Electric Double-Layer Capacitors (EDLCs). This sophisticated architecture facilitates a higher surface area-to-volume ratio, enabling efficient ion transport and charge storage. The nanofiber framework provides mechanical support while the aggregates create additional active sites for ion adsorption[27]. Porosity within the structure further enhances electrolyte accessibility and ion diffusion, optimizing charge storage capacity and rate capability. Consequently, this innovative design significantly improves the energy density, and power density, making them promising candidates for various energy storage applications[28].

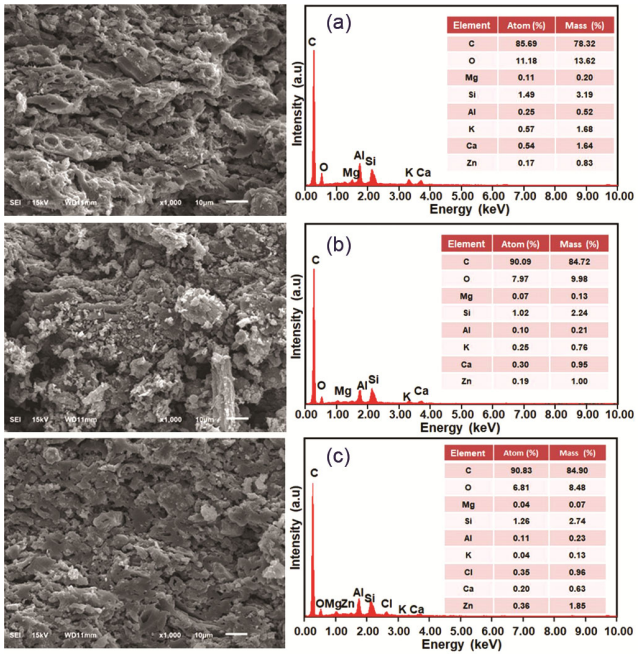

Fig. 4 — EDX spectrum of active materials (a) OPF-K, (b) OPF-N, and (c) OPF-Z

The EDX spectrum, as seen in Fig. 4, shows the distribution of chemical contents contained in the OPF active material. Each OPF active material contains the elements carbon, oxygen, and other small molecular substances such as magnesium (mg), silica (Si), aluminum (Al), potassium, calcium, zinc (Zn), and the element chlorine which is only found in OPF-Z, caused by the use of $ZnCl_2$ activator. The small molecule substance originates from the basic content of the Palm Oil Fiber biomass, where its presence is negligible. The carbon element is the dominant element in the OPF active material, which means that the KOH, $NiCl_2$, and $ZnCl_2$ activators have succeeded in reducing most hydrocarbon compounds, volatiles, or impurities during the carbonization process[29]. Furthermore, OPF-N has a higher carbon content than OPF-K and has a higher oxygen content than OPF-Z. This phenomenon proves that the $NiCl_2$ activator is superior compared to other activators when activated on palm oil fiber biomass. The combination of carbon and oxygen elements in the OPF-N material can respectively increase the electrical conductivity and wettability of the electrolyte which can support a better charge-discharge process and can improve the performance of supercapacitor cells[30].

The electrochemical properties of OPF-K, OPF-N, and OPF-Z were explored in a two-electrode system using CV and GCD methods in 1 M H_2SO_4 aqueous electrolyte. The CV curves for all samples can be seen

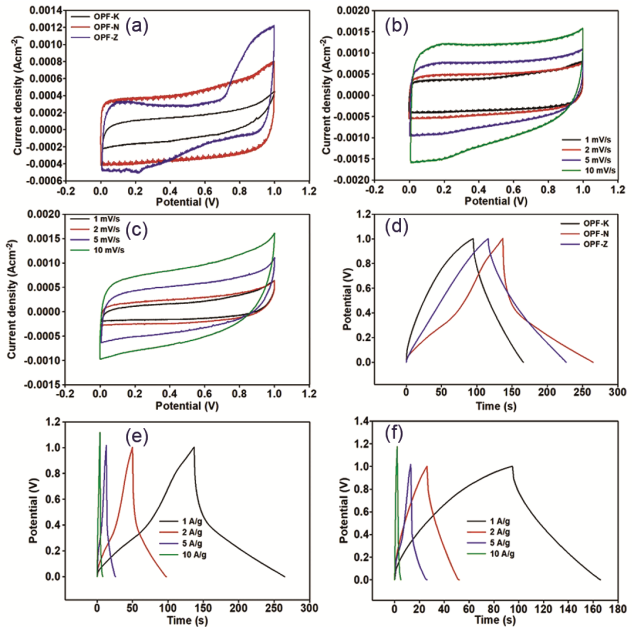

Fig. 5 — CV curve (a) OPF, (b) OPF-N, (c) OPF-Z, GCD curve (d) OPF, (e) OPF-N, and (f) OPF-Z

in Fig. 5(a), at a scan rate of 1 mV/s, having a quasi-rectangular shape confirming the presence of dominant EDLC behavior as well as a fast electrochemical response[31]. OPF-N exhibits quasi-rectangularity with the largest area, exhibiting the highest specific capacitance due to having an XRD-confirmed graphite structure with many more nanofibers and the presence of nanospheres and nanopores. Furthermore, OPF-N also has a higher SSAwith a high carbon content. The properties possessed by OPF-N are very useful in the accumulation of ion charges in the charge-discharge process, supporting the formation of more double-layer charges between the electrodes which can improve the performance of supercapacitor cells. The specific capacitance of each OPF active material is 66, 255, and 177 F/g for OPF-K, OPF-N and OPF-Z.

Figures. 5(b & c) show that increasing the scan rate from 1 to 10 mV/s leads to an enlargement of the voltammetric charge area on the CV curve[32]. This phenomenon is since a high scan rate can facilitate rapid charge adsorption–desorption, corresponding to a high current response and thus resulting in a larger CV profile. Furthermore, the CV curve of OPF still maintains a quasi-rectangular shape without any distortion, even at a high scan rate of 10 mV/s[33].

Figure 5(d) shows the electrochemical performance of the OPF material revealed using the GCD method at a potential of 0-1 V. The OPF active material has ideal EDLC characteristics which are characterized by the quasi-triangles formed[34]. OPF-N has longer charge and discharge times than OPF-K and OPF-Z, thus has better capacitive properties that are suitable for CV testing. Figures. 5(e & f) show the application of current density from 1 to 10 A/g in OPF-N and OPF-K supercapacitor cells, where the samples can maintain a quasi-triangular shape even at high current density. This indicates that the material has good electrochemical reversibility and high Coulomb efficiency[35].

4 Conclusion

This study provides a finding regarding the conversion of oil palm fiber (OPF) biomass into the active material for supercapacitor cells. OPF active material was synthesized by chemical activation using KOH, $ZnCl_2$, and $NiCL_2$ and double pyrolysis. At a scan rate of 1 mV/s, 255 F/g was obtained for the OPF-N sample, because it has the graphite structure shown in XRD, the presence of nanofibers, nanospheres, and nanopores shown in the carbon-rich SEM micrographs. These properties can increase the diffusion of electrolyte ions and electrical conductivity. The results of this study indicate that electrochemical performance improvement can be achieved by optimizing the activating agent during the chemical activation process. Furthermore, the production of active materials from palm oil midrib is very economical, abundantly available does not damage the environment, and can be produced on a large scale.

Acknowledgment

The authors are grateful to the DRPM Kemenristek/BRIN, Republic of Indonesia for financial support through first-year project of Penelitian Tesis Magister (PTM), with contract number: 15489/UN.19.5.1.3/AL.04/2023.

Reference

1 Fang J, Guo D, Kang C, Wan S, Li S, Fu L, Liu G & Liu Q, *IntJ Energy Res,* 43 (2019) 8811.
2 Zhang R, Hou Q, Wang Y, Zhu W, Fan J, Zheng M & Dong Q, *Electrochem Commun,* 139 (2022) 107310.
3 Liao H, Zhong L, Zeng H, Xiao Y, Cheng B & Lei S, *Carbon,* 213 (2023) 118305.
4 Selvaraj M, Balamoorthy E & Manivasagam T G, *J Energy Storage,* 72 (2023) 108543.
5 Farma R, Apriyani I, Awitdrus A, Taer E & Apriwandi A, *Sci Rep,*12 (2022) 1.
6 Farma R,Anugrah A P,Apriyani I & Awitdrus A, *Adv Natur Sci: Nanosci Nanotechnol,* 13 (2022).

7 Farma R, Apriyani I, Deraman M, Taer E, Nanda R & Sulistyo A, *J Energy Storage,* 67 (2023) 107611.
8 Gajalakshmi T, Kalaivani T, Chi N T L & Brindhadevi K, *Fuel,* 337 (2023) 2.
9 Sasono S R A, Rois M F, Widiyastuti W, Nurtono T & Setyawan H, *Res Eng,* 18 (2023) 101070.
10 Yan W, Siti-dina R P, Too S, Leng K & Er A C, *Environ Technol Innovat,* 30 (2023) 103050.
11 Yaro N S A, Sutanto M H, Habib N Z, Napiah M, Usman A, Jagaba A H & Al-Sabaeei A M, *J Road Eng,* 2 (2022) 309.
12 Zhang X, Han R, Liu Y, Li H, Shi W & Yan X, *Chem Eng J,* 460 (2023) 141607.
13 Gai L, Li J, Wang Q, Tian R & Li K, *J Environ Chem Eng,* 9 (2021) 106678.
14 Zhang X, Han R, Liu Y, Li H, Shi W, Yan X, Zhao X, Li Y & Liu B, *Chem Eng J,* 460 (2023) 141607.
15 Pecenek H, Kılıç F, Onses M S, Yılmaz E & Sahmetlioglu E, *J Energy Stor,* 64 (2023) 107075.
16 Hou L, Chen Z, Zhao Z, Sun X, Zhang J & Yuan C, *ACS Appl Energy Mater,*2 (2019) 548.
17 Wang L, Mu G, Tian C, Sun L, Zhou W, Yu P, Yin J & Fu H, *Chem Sus Chem,* 6 (2013) 880.
18 Kumari R, Singh V & Kant C R, *Mater Chem Phys,* 305 (2023) 127882.
19 Isaac R, Vitto M, Natividad M T & Palisoc S T, *J Power Sources,* 582 (2023) 233547.
20 Mehdi R, Naqvi S R, Khoja A H & Hussain R, *Fuel,* 348 (2023) 128529.
21 Balotin G, Almeida J D, Silva R S, Carvalho W A, Carvalho C T & Rodrigues R, *J Mol Catal,* 538 (2023) 112976.
22 Ouyang J, Wang X, Wang L, Xiong W, Li M, Hua Z, Zhao L, Zhou C, Liu X, Chen H & Luo Y, *Carbon,* 196 (2022) 532.
23 Ahmad T, Shaheen S, Khan S, Ali A, Ullah N, Oyama M & Aziz A, *Mater Sci Eng B,* 292 (2023)116430.
24 Pant B, Ojha G P, Acharya J & Park M, *Diamond Related Mater,* 136 (2023) 110040.
25 Gao Y, Wang J, Huang Y, Zhang S, Zhang S & Zou J, *Appl Surface Sci*, 638 (2023) 1.
26 Lin Y, Chen Z, Yu C & Zhong W, *Electrochim Acta,* 334 (2020) 135615.
27 Farma R, Simanjuntak S M & Apriyani I, *J Mater Sci: Mater Electron*, 34 (2023) 1. Farma R, Valensia I, Apriyani I, Deraman M, Awitdrus & Taer E, *J Electron Mater,* 53(2024) 1487.
28 Farma R, Indriani A & Apriyani I, *J Mater Sci: Mater Electron,* 34 (2023) 81.
29 Farma R, Husni H, Apriyani I, Awitdrus A & Taer E, *J Electron Mater,* 50 (2021) 6910.
30 Farma R, Apriyani I, Awitdrus A, Taer E & Apriwandi A, *Sci Rep,* 12 (2022) 1.
31 Farma R, Yunita A & Apriyani I, *Diamond Relat Mater,* 143 (2024) 110922.
32 Xu H, Zhang Y, Wang L, Chen Y & Gao S, *Renew Energy,* 179 (2021) 1826.
33 Ouyang D, Hu L, Wang G, Dai B, Yu F & Zhang L, *New Carbon Mater,* 36 (2021) 350.
34 Tu J, Qiao Z, Wang Y, Li G, Zhang X, Li G & Ruan D, *Int J Electrochem Sci,* 18 (2023) 16.